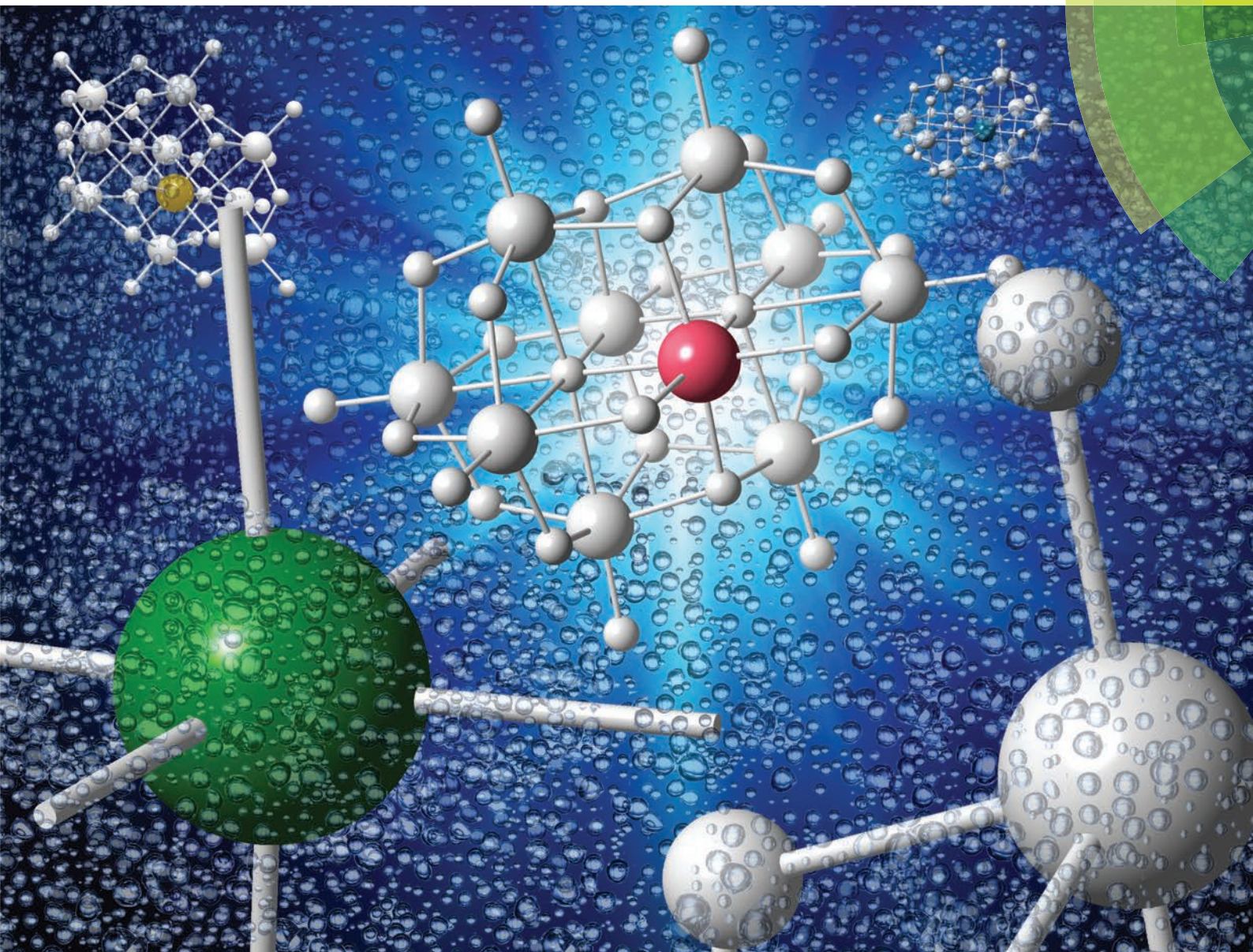


# Dalton Transactions

An international journal of inorganic chemistry

[www.rsc.org/dalton](http://www.rsc.org/dalton)



ISSN 1477-9226



**PAPER**

Jung-Ho Son, William H. Casey *et al.*  
Structure, stability and photocatalytic H<sub>2</sub> production by Cr-, Mn-, Fe-, Co-, and Ni-substituted decanobate clusters





Cite this: *Dalton Trans.*, 2014, **43**, 17928

## Structure, stability and photocatalytic H<sub>2</sub> production by Cr-, Mn-, Fe-, Co-, and Ni-substituted decaniobate clusters†

Jung-Ho Son,<sup>\*a</sup> Jiarui Wang<sup>a</sup> and William H. Casey<sup>\*a,b</sup>

Received 3rd July 2014,  
Accepted 29th July 2014  
DOI: 10.1039/c4dt02020k

www.rsc.org/dalton

Here we report synthesis and characterization of early transition-metal(TM)-substituted decaniobates as a continuation of our previous report of tetramethylammonium (TMA) salt of FeNb<sub>9</sub> and NiNb<sub>9</sub>: TMA<sub>6</sub>[H<sub>2</sub>Cr<sup>III</sup>Nb<sub>9</sub>O<sub>28</sub>]·14H<sub>2</sub>O (**1**, CrNb<sub>9</sub>), TMA<sub>8</sub>[Mn<sup>III</sup>Nb<sub>9</sub>O<sub>28</sub>]·29H<sub>2</sub>O (**2**, MnNb<sub>9</sub>) and TMA<sub>7</sub>[H<sub>2</sub>Co<sup>II</sup>Nb<sub>9</sub>O<sub>28</sub>]·25H<sub>2</sub>O (**3**, CoNb<sub>9</sub>). Among the TM-substituted decaniobates, CoNb<sub>9</sub> or NiNb<sub>9</sub> exhibit a higher photocatalytic H<sub>2</sub> evolution activity in methanol–water mixtures than others.

Early transition-metal (TM) substituted Keggin-type polyoxometalates have been studied for decades because of their rich electrochemical, optical, magnetic and catalytic properties.<sup>1</sup> In group 5 polyoxometalate chemistry, decametate ions with *D*<sub>2v</sub> symmetry, such as decavanadate and decaniobate (Nb<sub>10</sub>) ions, are well known,<sup>2</sup> but TM-substituted decametates are rare, although Ti<sup>IV</sup>-, Fe<sup>III</sup>-, Ni<sup>II</sup>-substituted decaniobates (henceforth denoted: FeNb<sub>9</sub> and NiNb<sub>9</sub>, respectively) and Pt-substituted decavanadate have been synthesized.<sup>3</sup> Herein we describe the synthesis of the Cr-, Mn-, and Co-substituted decaniobates, and examine the trend in the structural, magnetic, optical, and photocatalytic H<sub>2</sub>-evolution properties of the TM-substituted decaniobates exhibit different stabilities and ease of synthesis that seem to be relatable to their structures. Moreover, the clusters show photocatalytic H<sub>2</sub>-evolution, with Ni- and Co-substituted decaniobate ions being more active than other substituted decaniobates, although the molecules partly dissociate during irradiation into the corresponding MO<sub>x</sub> and niobate. The results can aid the understanding of the factors governing the photocatalytic H<sub>2</sub>-evolution properties of TM-doped metal oxides, including titanates,<sup>4</sup> other niobates,<sup>5</sup> and related polyoxoniobate systems.<sup>6</sup>

Isolation of tetramethylammonium (TMA) salts of Cr-, Mn- and Co-substituted decaniobates in this paper, TMA<sub>6</sub>[H<sub>2</sub>Cr<sup>III</sup>Nb<sub>9</sub>O<sub>28</sub>]·14H<sub>2</sub>O (**1**, CrNb<sub>9</sub>), TMA<sub>8</sub>[Mn<sup>III</sup>Nb<sub>9</sub>O<sub>28</sub>]·29H<sub>2</sub>O (**2**, MnNb<sub>9</sub>) and TMA<sub>7</sub>[H<sub>2</sub>Co<sup>II</sup>Nb<sub>9</sub>O<sub>28</sub>]·25H<sub>2</sub>O (**3**, CoNb<sub>9</sub>) was more challenging than our previously work on the Fe- and Ni-substituted decaniobates.<sup>3d</sup> We noticed that in the chromium-substitution reaction, CrNb<sub>9</sub> coexisted with previously reported [Cr<sub>2</sub>(OH)<sub>4</sub>Nb<sub>10</sub>O<sub>30</sub>]<sup>8-</sup> (Cr<sub>2</sub>Nb<sub>10</sub>) in most of the syntheses.<sup>7</sup> These structurally distinct clusters were separable by taking advantage of their slightly different solubility. Firstly, TMA salt of Cr<sub>2</sub>Nb<sub>10</sub> was extracted with ethanol, and remaining TMA salt of CrNb<sub>9</sub>–Nb<sub>10</sub> mixture was extracted with ethanol–methanol to yield an extract of **1**. Crystallization of **2** and **3** were challenging because of the slow decomposition of MNb<sub>9</sub> (M = Mn or Co) to Nb<sub>10</sub> in the viscous liquid product. The color of the oily product changed from purple to brown (MnNb<sub>9</sub>) and pink to blue (CoNb<sub>9</sub>) during the crystallization attempt, concomitant with Nb<sub>10</sub> crystal formation. This observation suggests decomposition of MNb<sub>9</sub> cluster and oxidation of the corresponding released transition metal oxide (M = Mn or Co) by O<sub>2</sub> in air. However, we were able to isolate decent amount of MnNb<sub>9</sub> and CoNb<sub>9</sub> crystals (28 and 45% yields, respectively) by cooling the concentrated ethanolic solution after extraction. Decomposition of Mn- and Co-substituted decaniobate structures during storage was avoided by prompt filtration by washing with ethanol, followed by drying and storage *in vacuo*. On the other hand, Cr-, Fe- or Ni-substituted decaniobate ions did not decompose noticeably either during the long crystallization step in a viscous liquid product or upon storage in air.

Electrospray-ionization mass spectrometry (ESI-MS) was used to determine the identities of substituted decaniobates [Fig. 2]. The purified samples were dissolved in water for

<sup>a</sup>Department of Chemistry, University of California, Davis, One Shields Ave., Davis, CA 95616, USA. E-mail: junghoson@gmail.com, whcasey@ucdavis.edu; Fax: +1 530 752 8995; Tel: +1 530 752 3211

<sup>b</sup>Department of Geology, University of California, Davis, One Shields Ave., Davis, CA 95616, USA

†Electronic supplementary information (ESI) available: ESI-MS and UV-Vis titration data, magnetism data, detailed H<sub>2</sub> evolution data with change of solution speciation by ESI-MS, UV-Vis, and TEM/EDS data of the colloids after irradiation. CCDC 990475, 990476 and 990477. For ESI and crystallographic data in CIF or other electronic format see DOI: 10.1039/c4dt02020k



ESI-MS analyses. ESI-MS of **1–3** shows peaks in the lower  $m/z$  region compared to  $\text{Nb}_{10}$  due to the substitution of one  $\text{Nb}^{\text{V}}$  site with an early TM of lower atomic mass than niobium. ESI-MS also indicates a single-site substitution, as was confirmed by X-ray crystallography (*vide infra*). We find no evidence of multiple site substitution, in spite of exploration of other reagent stoichiometries and/or different reaction temperatures.

Structures of the substituted decaniobate clusters with Cr, Mn and Co substituents were determined by X-ray single crystallography. The results show that the substitution occurred exclusively at the central site of the decaniobate moiety, similar to other substituted decaniobate structures ( $\text{M} = \text{Ti}, \text{Fe}, \text{Ni}$ ) [Fig. 1].<sup>3</sup> Bond-valence sum (BVS) calculations of metal centres suggest the oxidation state of the metals as  $\text{Cr}^{\text{III}}$  (2.86 and 2.90),  $\text{Mn}^{\text{III}}$  (3.07) and  $\text{Co}^{\text{II}}$  (1.92) [Table S1†]. We note that some  $\text{Mn}^{\text{IV}}$ -included heteropolyniobate clusters have been reported previously.<sup>8</sup> Numbers of TMA counteranions found in the crystal structures of **1–3** are 6, 8 and 7, respectively, and these numbers agree well with the elemental analysis results. Thus the formulae of the clusters in **1–3** can be expressed as  $[\text{H}_2\text{Cr}^{\text{III}}\text{Nb}_9\text{O}_{28}]^{6-}$ ,  $[\text{Mn}^{\text{III}}\text{Nb}_9\text{O}_{28}]^{8-}$  and  $[\text{H}_2\text{Co}^{\text{II}}\text{Nb}_9\text{O}_{28}]^{7-}$ , respectively. In the  $\text{CrNb}_9$  structure, two protons are found on the two  $\mu_2\text{-O}$  atoms between Cr and Nb. Protons were not found in the electron-density map of the  $\text{CoNb}_9$  structure, but BVS calculation of the two  $\mu_2\text{-O}$  bound to Co (0.983 and 1.013) suggests that two  $\mu_2\text{-O}$  between Co and Nb are protonated, as in the  $\text{CrNb}_9$  molecule. In  $\text{MnNb}_9$  structure, BVS values of all Mn-bound oxygen atoms are higher than 1.5, supporting a conclusion that  $\text{MnNb}_9$  is not protonated. While  $\text{Cr}^{\text{III}}$  and  $\text{Co}^{\text{II}}$  retained their oxidation state from the source reagent,  $\text{Mn}^{\text{II}}$  from the reagent was oxidized to  $\text{Mn}^{\text{III}}$  in the cluster, which might have happened in the hydrothermal synthesis condition.



Fig. 1 Polyhedral model of  $\text{MNb}_9$  clusters ( $\text{M} = \text{Cr}^{\text{III}}, \text{Mn}^{\text{III}}$  and  $\text{Co}^{\text{II}}$ , from top to bottom) in **1–3** (white: Nb, green: Cr, purple: Mn, pink: Co).

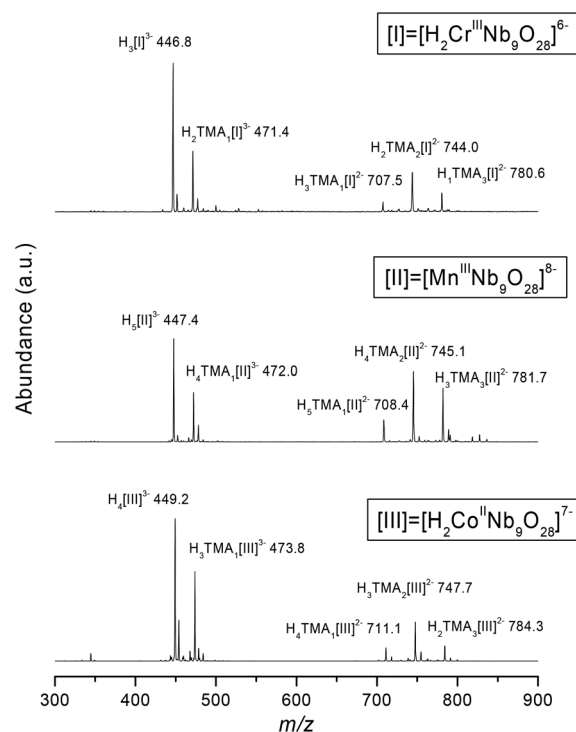


Fig. 2 ESI-MS of compounds **1–3** dissolved in water (from top to bottom).

Enough of these  $\text{MNb}_9$  structures are now available to compare the  $\text{M-O}$  bond lengths [Fig. 3]. We find that the  $\text{M-}\mu_6\text{-O}$  and  $\text{M-}\mu_2\text{-O}$  lengths increase from Cr to Co then decrease slightly for the Ni-substituted molecule. This trend is similar to the Shannon's ionic radii of the TM ion series.<sup>9</sup> We speculate that a discrepancy in this trend for  $\text{MnNb}_9$  is due to the disordered central site with half occupancy of Nb in the structure of  $\text{MnNb}_9$ . We point out that two axial *trans*  $\text{M-}\mu_3\text{-O}$  bonds are asymmetric in Cr, Fe and Ni derivatives of the

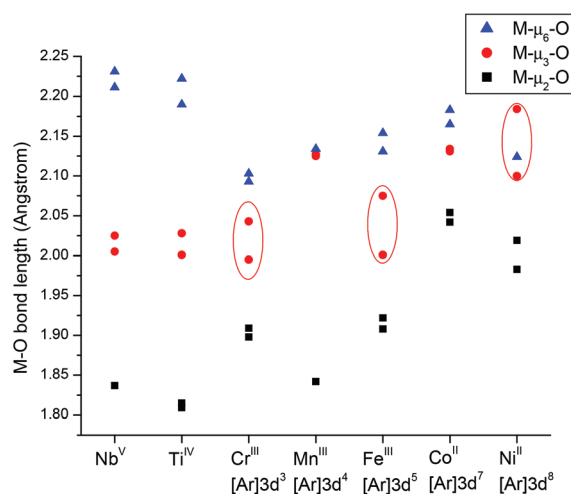
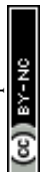


Fig. 3 The central  $\text{M-O}$  bond lengths in decaniobate and TM-substituted decaniobates. X-axis shows corresponding central atoms and their electron configurations.



MNb<sub>9</sub>, while those in Mn- and Co-substituted MNb<sub>9</sub> are more symmetric [Fig. 3]. Larger differences in the axial *trans* M-μ<sub>3</sub>-O bond lengths are observed as the group number of the substituted metal increases. (The red stretched circles are shown the same size to better indicate how asymmetry increases as one moves to the right in Fig. 3.) We note that clusters with large asymmetry in the axial M-μ<sub>3</sub>-O bonds have greater stability than clusters with symmetric M-μ<sub>3</sub>-O bonds lengths: MnNb<sub>9</sub> and CoNb<sub>9</sub> slowly decomposed to Nb<sub>10</sub> in the viscous crude product, as described above. The correlation is interesting but inconclusive and but immediately suggests a useful computational study.

An ESI-MS titration of 2 mM solutions of each cluster was performed to compare the stabilities of the substituted decaniobates as a function of pH [Fig. S1–S3†]. The varying intensity of the strongest peak of each ESI-MS data (445–450 *m/z*) was plotted to evaluate the stability of each substituted decaniobate clusters according to pH [Fig. 4]. While 1–3 show similarly decreasing peak abundance above pH 11 in the base titration, which suggests decomposition, a different trend is evident in the acid titration. CoNb<sub>9</sub> forms a precipitate immediately upon adding a small amount of acid, as we have found previously in the titration of FeNb<sub>9</sub> and NiNb<sub>9</sub>.<sup>3d</sup> However, MnNb<sub>9</sub> and CrNb<sub>9</sub> did not readily precipitate by adding acid; titration of MnNb<sub>9</sub> and CrNb<sub>9</sub> with acid exhibited some buffering and significant precipitation only occurred below pH 5.3 and pH 4.7, respectively. Although the stabilities are broadly similar across the series [Fig. 4], the stability window in acidic region is CrNb<sub>9</sub> > MnNb<sub>9</sub> > Fe ≈ Co ≈ NiNb<sub>9</sub>.

A purified sample of 1 has a lighter green color relative to the dark turquoise (bluish green) of [Cr<sub>2</sub>Nb<sub>10</sub>O<sub>34</sub>]<sup>8–</sup>, both in solution and solid. Crystals of 2 are deep purple and those of 3 are violet. The UV-Vis spectra of 1–3 during titration with TMAOH solution are shown in Fig. S4–S6†. The solution of 1 shows absorption at 450 and 650 nm from <sup>4</sup>A<sub>2g</sub>(F)→<sup>4</sup>T<sub>1g</sub>(F) and <sup>4</sup>A<sub>2g</sub>(F)→<sup>4</sup>T<sub>2g</sub>(F) transitions, respectively [Fig. S4†].<sup>10</sup> Different electronic transitions from light absorption are responsible for the slightly different colors of CrNb<sub>9</sub> and Cr<sub>2</sub>Nb<sub>10</sub>, as CrNb<sub>9</sub> is absorbing at 650 nm, while Cr<sub>2</sub>Nb<sub>10</sub> shows absorption at

600 nm.<sup>7</sup> During the titration of 1 with base, the two absorption maxima at 450 and 650 nm start to shift to 470 and 670 nm above pH 9 and a new absorption at 320 nm becomes evident. Titration coupled to ESI-MS indicated that significant decomposition only occurred above pH ~ 11 [Fig. 4 and Fig. S1†]. We thus suggest that the change of spectral profile of CrNb<sub>9</sub> above pH 9 is more likely due to deprotonation than decomposition, although this conclusion is speculative. A solution of 2 exhibits a broad absorption at 550 nm, which can be assigned to <sup>5</sup>E<sub>g</sub>→<sup>5</sup>T<sub>2g</sub> transition of Mn<sup>III</sup> [Fig. S5†].<sup>10</sup> The natural pH attained by a 2 mM solution of 2 is relatively high (~10), compared to 1 (pH 6.7) and 3 (pH 8.6), indicating a higher proton affinity. During the base titration of 2, an isosbestic point was observed around pH 11. A solution of 3 shows absorption at 500 and 545 nm (<sup>4</sup>T<sub>1g</sub>(F)→<sup>4</sup>T<sub>1g</sub>(P) transition), which is a similar feature in the [Co(H<sub>2</sub>O)<sub>6</sub>]<sup>2+</sup> ion [Fig. S6†].<sup>10</sup> The spectra of CoNb<sub>9</sub> did not change significantly until pH ~ 12, which is similar to the behavior found in UV-Vis titrations of FeNb<sub>9</sub> and NiNb<sub>9</sub>.<sup>3d</sup>

The magnetic measurements satisfy the Curie law, as can be seen from the almost linear 1/χ<sub>m</sub> vs. temperature plot of each compound [Fig. S7†]. Thus the compounds are paramagnetic, as is expected given that the clusters each contain a single isolated TM in otherwise diamagnetic niobate framework. The Curie constants derived by curve fitting χ<sub>m</sub> vs. temperature plot are presented in Table S2.† Fig. 5 shows the effective magnetic moments (μ<sub>eff</sub>) of the series as a function of temperature. The μ<sub>eff</sub> values of each compound at their maxima are close to typical experimental μ<sub>eff</sub> values for compounds with single corresponding TM ion in high-spin configuration (*i.e.* 3.8, 4.9, 5.9, 4.8, 3.2 for Cr<sup>III</sup>, Mn<sup>III</sup>, Fe<sup>III</sup>, Co<sup>II</sup>, Ni<sup>II</sup>, respectively),<sup>11</sup> confirming the single-site substitution, the assigned oxidation states and high-spin states of the heterometals. However, the μ<sub>eff</sub> values of all compounds slightly decrease with increasing temperature, which might be due to the spin disorder at higher temperatures. We note that FeNb<sub>9</sub> and CrNb<sub>9</sub> have maximum μ<sub>eff</sub> around 7 K. On the other hand, NiNb<sub>9</sub>, MnNb<sub>9</sub> and CoNb<sub>9</sub> show maxima at 20 K, 35 K and 120 K, respectively. The sharp decrease of μ<sub>eff</sub> of Ni<sup>II</sup> and Mn<sup>III</sup>

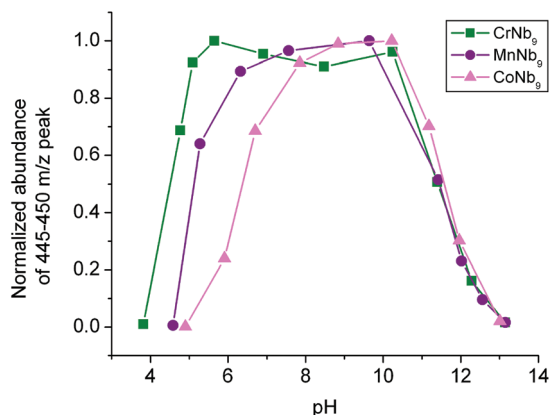


Fig. 4 Normalized peak intensity (strongest peak) in ESI-MS of 1–3 as a function of pH, based on Fig. S1–S3.†

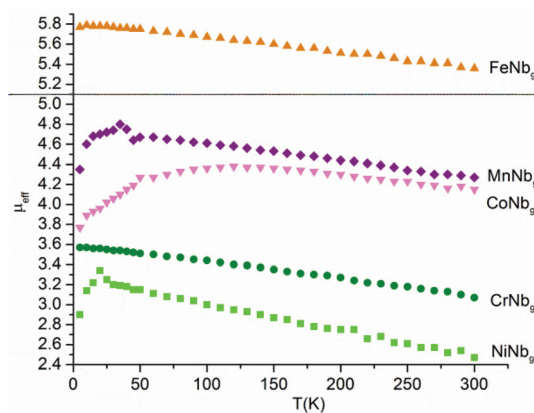


Fig. 5 μ<sub>eff</sub> vs. temperature for TMA salts of TM-substituted decaniobates.



compounds in the low-temperature region is known to be due to zero-field splitting.<sup>12</sup> The gradual decrease of  $\mu_{\text{eff}}$  for the  $\text{Co}^{\text{II}}$ -substituted decaniobate at lower temperatures has been observed for other  $\text{Co}^{\text{II}}$  compounds, and is generally attributed to spin-orbit coupling.<sup>12</sup>

TM-doped polyoxometalate clusters have recently been shown to possess electrocatalytic properties for water oxidation.<sup>13</sup> To test the ability of the niobate clusters to act as photocatalysts for  $\text{H}_2$  evolution, irradiation tests were conducted. For the experiment, 50 mg of each compound was dissolved in mixed solution of methanol and water (50 mL, 20% v/v, methanol as sacrificial oxidant). Visible-light irradiation by using UV filter (cut-off wavelength  $<400$  nm) on the sample solutions showed no appreciable  $\text{H}_2$  evolution, indicating that the electron-hole pairs created by excitation of the TMs by visible light are not accessible for redox reactions on the cluster surface. However, irradiation with the full spectrum of the Xe lamp produced significant amounts of  $\text{H}_2$ .  $\text{NiNb}_9$  and  $\text{CoNb}_9$  showed  $\sim 4$  times higher  $\text{H}_2$  evolution than  $\text{Nb}_{10}$  [Fig. S8†].  $\text{FeNb}_9$ ,  $\text{MnNb}_9$  and  $\text{CrNb}_9$  showed similar or lower activity than  $\text{Nb}_{10}$ . ESI-MS of the solutions after irradiation indicated that a significant amount of each cluster had decomposed to hexaniobate and  $\text{Nb}_{10}$  during irradiation. To explain the nature of active photocatalyst, we carried out  $\text{H}_2$ -evolution experiments using higher cluster concentrations.

When the  $\text{H}_2$ -evolution experiment was performed with four-times higher cluster concentration (*i.e.* with 0.2 g of sample in 50 mL MeOH-water, 20% v/v; 1.6 to 2.0 mM), similar trends were found, with  $\text{NiNb}_9$  ( $217 \mu\text{mol g}^{-1} \text{h}^{-1}$ ) and  $\text{CoNb}_9$  ( $214 \mu\text{mol g}^{-1} \text{h}^{-1}$ ) showing higher  $\text{H}_2$ -evolution activity than the other clusters, which was generally similar or lower than  $\text{Nb}_{10}$  ( $59 \mu\text{mol g}^{-1} \text{h}^{-1}$ ) [Fig. 6]. The non-linearly increasing  $\text{H}_2$ -evolution rate of both  $\text{NiNb}_9$  and  $\text{CoNb}_9$  suggests formation of photocatalytically active forms from consumption or dissociation of original cluster. The color of the solutions changed after irradiation [Fig. S9†] and the solution exhibited scattering of laser light by colloids. Overall absorbance in UV-Vis spectra of the solutions increased after irradiation,

which is also consistent with the formation of metal-oxide colloids upon irradiation [Fig. S10†]. ESI-MS indicated that a large portion of the  $\text{MNb}_9$  clusters in solutions decomposed after irradiation to hexaniobate and  $\text{Nb}_{10}$ , but some  $\text{MNb}_9$  still remained [Fig. S11†]. Similarly, we observed photodecomposition of the Te-substituted Lindqvist-type niobate clusters into hexaniobate and metallic tellurium nanowires, which showed high  $\text{H}_2$ -evolution activity.<sup>14</sup> High  $\text{H}_2$ -evolution activity from  $\text{NiNb}_9$  is not surprising, since Ni-doped  $\text{K}_4\text{Nb}_6\text{O}_{17}$  showed much higher  $\text{H}_2$ -evolution activity compared to other early TM- (from Cr to Cu) doped  $\text{K}_4\text{Nb}_6\text{O}_{17}$ .<sup>5</sup> The high  $\text{H}_2$ -evolution activity of Ni-loaded  $\text{K}_4\text{Nb}_6\text{O}_{17}$  was attributed to segregated NiO nanoparticles on  $\text{K}_4\text{Nb}_6\text{O}_{17}$  sheets.<sup>15</sup> Thus the high activity of  $\text{NiNb}_9$  could similarly be attributed to formation of  $\text{Ni}^0$  or  $\text{NiO}_x$  particles and their interaction with niobates. Niobate will generate electron-hole pairs upon UV light irradiation<sup>16</sup> and  $\text{Ni}^0/\text{NiO}_x$  particle will reduce protons, producing  $\text{H}_2$ . We note that whether  $\text{Ni}^0$ , or  $\text{NiO}_x$ , or both, are the active cocatalyst is controversial; we cannot contribute to this discussion here.<sup>17</sup>

Upon irradiation,  $\text{CoNb}_9$  solutions exhibited  $\text{H}_2$ -evolution curves that were similar to  $\text{NiNb}_9$  solution [Fig. 6]. ESI-MS spectrum after irradiation indicated that a solution of  $\text{CoNb}_9$  is still dominated by the  $\text{CoNb}_9$  ion, but the UV-Vis spectra had changed, indicating some decomposition [Fig. S10 and S11†]. The appreciable activity of  $\text{CoNb}_9$  in photocatalytic  $\text{H}_2$ -evolution is interesting because Co-doped  $\text{K}_4\text{Nb}_6\text{O}_{17}$  showed much lower  $\text{H}_2$ -evolution activity compared to Ni-doped  $\text{K}_4\text{Nb}_6\text{O}_{17}$ .<sup>5</sup> Hill *et al.* remarked that the distinction between homogeneous and heterogeneous catalysis is elusive for their Co-doped polyoxotungstate catalytic systems, and that is certainly also true here for the substituted niobates.<sup>18</sup>

The  $\text{H}_2$ -evolution activity of the cluster solution depends on pH. A large amount of light grey precipitate formed after irradiating the  $\text{NiNb}_9$  solution when the pH was lowered before irradiation, and this solution showed enhanced  $\text{H}_2$ -evolution activity upon irradiation, with a distinct nonlinear curve ( $986 \mu\text{mol g}^{-1} \text{h}^{-1}$ ) [Fig. S12†]. No clusters remained in the solution after irradiation, as indicated by ESI-MS. The pH after irradiation was 5.8, much lower than natural pH of a solution formed from freshly dissolved solid, and is instead consistent with extensive hydrolysis reactions upon irradiation, leading to proton release and precipitation. Transmission-electron microscopy (TEM) images of the precipitate showed agglomerated nanoparticles ( $<10$  nm), and the composition is about Ni : Nb = 1 : 8.7, as determined by energy-dispersive X-ray spectroscopy (EDS) [Fig. S13†], which is close to the cluster composition. This result suggests that the nanoparticles are composed of  $\text{NiO}_x$  and  $\text{NbO}_x$ , but phase distinction was not possible due to resolution limit. Powder X-ray diffraction of this precipitate indicated no crystallinity. One hypothesis is that, by forcing precipitation at low pH, the  $\text{NiNb}_9$  system exhibited a higher  $\text{H}_2$ -evolution because the colloids were catalytic. Interestingly,  $\text{CoNb}_9$  exhibited an opposite trend [Fig. S12†]. The  $\text{H}_2$ -evolution activity of  $\text{CoNb}_9$  was nearly lost after precipitate formed by lowering the pH, which suggests

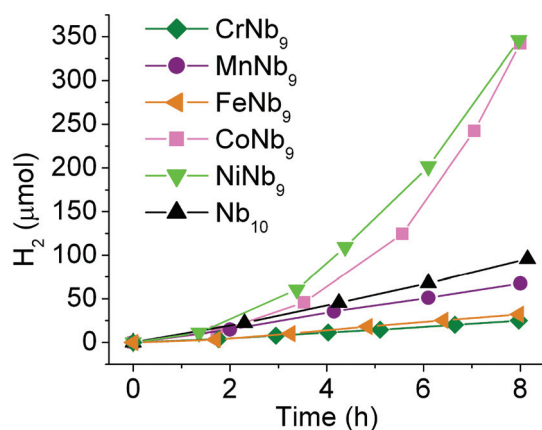


Fig. 6  $\text{H}_2$ -evolution upon Xe-lamp irradiation of 0.2 g of TM-substituted decaniobate TMA salts in 50 mL MeOH- $\text{H}_2\text{O}$  solution (20% v/v).





that H<sub>2</sub> evolution in CoNb<sub>9</sub> solution may be from cluster ions and not the colloids.

## Conclusions

Early TM-substituted (from group 6 to 10) decaniobate ions have differences in their solid-state structure that can be related to their stability and properties. The range of widely varying stabilities of the clusters is a key challenge in the synthesis and purification of this series of polyoxoniobates. We suggest that the higher H<sub>2</sub>-evolution activity from the Ni- and Co-substituted decaniobate ions arises *via* separate heterogeneous (Ni) and homogeneous (Co) routes, but in any case is only evident during UV irradiation. Their increased activity is attributed to cocatalysis from the photodecomposition products, most likely as Ni<sup>0</sup> and Ni oxide, and Co hydroxide, with amorphous Nb<sub>2</sub>O<sub>5</sub> or with the niobate cluster in solution. CoNb<sub>9</sub> is interesting because a relatively larger amount of the cluster ions survive irradiation.

## Experimental details

### Synthesis of 1 (CCDC 990475)

Hydrous niobium oxide (5 g, 80% w/w) was mixed with 0.89 g of CrCl<sub>3</sub>·6H<sub>2</sub>O in a 23 mL capacity PTFE-lined autoclave and 5.5 g of TMAOH·6H<sub>2</sub>O was added. The mixture was reacted at 110 °C for 4 days. Reaction mixture solution was washed with isopropanol in a plastic centrifuge tube (50 mL) several times until the sticky product remained. The product was extracted with ethanol until extract was nearly colorless. Ethanol extract was discarded and remaining green precipitate was extracted with methanol–ethanol (*ca.* 1 : 1) solution. Crystalline product was obtained after evaporation. Yield = 1.9 g (28%). Elemental analysis Found: C 14.34, H 5.19, N 4.06, Cr 2.34, Nb 38.40. Calcd for C<sub>24</sub>H<sub>102</sub>N<sub>6</sub>CrNb<sub>9</sub>O<sub>42</sub>: C 14.15, H 5.05, N 4.13, Cr 2.56, Nb 41.09.

### Synthesis of 2 (CCDC 990476)

Hydrous niobium oxide (5 g, 80% w/w) was mixed with 0.66 g of MnCl<sub>2</sub>·4H<sub>2</sub>O in a 23 mL capacity PTFE-lined autoclave and 5.5 g of TMAOH·6H<sub>2</sub>O was added. The mixture was reacted at 110 °C for 4 days. Reaction mixture solution was washed with isopropanol in a plastic centrifuge tube (50 mL) several times until the sticky product remained. The product was extracted with ethanol (*ca.* 200 mL). The ethanolic solution was concentrated to less than 50 mL by using rotary evaporator and kept in a freezer. Dark purple rod-like crystals formed. The product crystals were quickly filtered on a frit and washed with minimum amount of ethanol, and dried *in vacuo*. Yield = 2.3 g (28%). Elemental analysis Found: C 15.39, H 5.99, N 4.41, Mn 2.19, Nb 34.10. Calcd for C<sub>32</sub>H<sub>154</sub>N<sub>8</sub>MnNb<sub>9</sub>O<sub>57</sub>: C 15.65, H 6.32, N 4.56, Mn 2.24, Nb 34.07.

### Synthesis of 3 (CCDC 990477)

Hydrous niobium oxide (5 g, 80% w/w) was mixed with 0.8 g of CoCl<sub>2</sub>·6H<sub>2</sub>O in a 23 mL capacity PTFE-lined autoclave and 5.5 g of TMAOH·6H<sub>2</sub>O was added. The mixture was reacted at 110 °C for 4 days. Reaction mixture solution was washed with isopropanol in a plastic centrifuge tube (50 mL) several times until the sticky product remained. The product was extracted with ethanol (*ca.* 200 mL). The ethanolic solution was concentrated to less than 50 mL by using rotary evaporator and kept in a freezer. Pale violet needle-like crystals formed were quickly filtered on a frit and washed with minimum amount of ethanol and dried *in vacuo*. Yield = 3.5 g (45%). Elemental analysis Found: C 14.53, H 6.01, N 4.44, Co 2.50, Nb 34.30. Calcd for C<sub>28</sub>H<sub>136</sub>N<sub>7</sub>CoNb<sub>9</sub>O<sub>53</sub>: C 14.52, H 5.92, N 4.24, Co 2.55, Nb 36.14.

### Crystal data

(1) CCDC 990475. C<sub>24</sub>H<sub>93</sub>N<sub>6</sub>Cr<sub>1.03</sub>Nb<sub>8.98</sub>O<sub>42.44</sub>, *M* = 2032.17, monoclinic, *a* = 16.6016(8), *b* = 17.2436(8), *c* = 24.0263(11) Å, β = 106.121(1)°, *U* = 6607.6(5) Å<sup>3</sup>, *T* = 93 K, space group *P*2<sub>1</sub>/*n* (no. 14), *Z* = 4, 66308 reflections measured, 13 488 unique (*R*<sub>int</sub> = 0.0218) which were used in all calculations. The final *wR*(*F*<sup>2</sup>) was 0.0656 (all data). (2) CCDC 990476. C<sub>33.60</sub>H<sub>60</sub>N<sub>8</sub>Mn<sub>1.04</sub>Nb<sub>8.96</sub>O<sub>56.90</sub>, *M* = 2376.48, monoclinic, *a* = 22.846(6), *b* = 13.767(4), *c* = 17.970(5) Å, β = 129.353(4)°, *U* = 4370(2) Å<sup>3</sup>, *T* = 93 K, space group *C*2/*m* (no. 12), *Z* = 2, 23936 reflections measured, 5199 unique (*R*<sub>int</sub> = 0.0138) which were used in all calculations. The final *wR*(*F*<sup>2</sup>) was 0.1285 (all data). (3) CCDC 990477. C<sub>28</sub>H<sub>72</sub>N<sub>7</sub>CoNb<sub>9</sub>O<sub>53</sub>, *M* = 2250.05, monoclinic, *a* = 25.543(2), *b* = 13.8124(12), *c* = 23.383(2) Å, β = 104.026(1)°, *U* = 8003.9(12) Å<sup>3</sup>, *T* = 88 K, space group *P*2<sub>1</sub>/*c* (no. 14), *Z* = 4, 126087 reflections measured, 24 416 unique (*R*<sub>int</sub> = 0.0315) which were used in all calculations. The final *wR*(*F*<sup>2</sup>) was 0.1700 (all data).

## Acknowledgements

This work was supported by an NSF CCI grant through the Center for Sustainable Materials Chemistry, number CHE-1102637. We thank Prof. Frank E. Osterloh for useful discussions. We thank Aimee Brian and Peter Klavins for magnetic property measurements, and Prof. Kirill Kovnir for discussion about magnetism data.

## Notes and references

- (a) L. C. W. Baker, V. S. Baker, K. Eriks, M. T. Pope, M. Shibata, O. W. Rollins, J. H. Fang and L. L. Koh, *J. Am. Chem. Soc.*, 1966, **88**, 2329; (b) L. C. W. Baker and J. S. Figgis, *J. Am. Chem. Soc.*, 1970, **92**, 3794–3797; (c) T. J. R. Weakley, *J. Chem. Soc., Dalton Trans.*, 1973, 341–346; (d) C. L. Hill and R. B. Brown Jr., *J. Am. Chem. Soc.*, 1986, **108**, 536–538; (e) M. Faraj and C. L. Hill, *J. Chem. Soc., Chem. Commun.*, 1987, 1487–1489; (f) J. Hu and



- R. C. Burns, *J. Mol. Catal. A: Chem.*, 2002, **184**, 451–464; (g) J.-H. Choi, J. K. Kim, D. R. Park, T. H. Kang, J. H. Song and I. K. Song, *J. Mol. Catal. A: Chem.*, 2013, **371**, 111–117.
- 2 M. T. Pope, *Heteropoly and Isopolyoxometalates*, Springer Verlag, Berlin, 1983.
  - 3 (a) M. Nyman, L. J. Criscenti, F. Bonhomme, M. A. Rodriguez and R. T. Cygan, *J. Solid State Chem.*, 2003, **176**, 111–119; (b) U. Lee, H.-C. Joo, K.-M. Park, S. S. Mal, U. Kortz, B. Keita and L. Nadjo, *Angew. Chem., Int. Ed.*, 2008, **47**, 793–796; (c) C. A. Ohlin, E. M. Villa, J. C. Fettinger and W. H. Casey, *Dalton Trans.*, 2009, 2677–2678; (d) J.-H. Son, C. A. Ohlin and W. H. Casey, *Dalton Trans.*, 2013, **42**, 7529–7533.
  - 4 (a) A. Fujishima and K. Honda, *Nature*, 1972, **238**, 37–38; (b) D. W. Hwang, H. G. Kim, J. S. Jang, S. W. Bae, S. M. Ji and J. S. Lee, *Catal. Today*, 2004, **93**, 845–850; (c) R. Niishiro, H. Kato and A. Kudo, *Phys. Chem. Chem. Phys.*, 2005, **7**, 2241–2245; (d) P. D. Tran, L. Xi, S. K. Batabyal, L. H. Wong, J. Barber and J. S. C. Loo, *Phys. Chem. Chem. Phys.*, 2012, **14**, 11596–11599; (e) H. Yu, S. Ouyang, S. Yan, Z. Li, T. Yua and Z. Zou, *J. Mater. Chem.*, 2011, **21**, 11347–11351; (f) R. Dholam, N. Patel, M. Adami and A. Miotello, *Int. J. Hydrogen Energy*, 2009, **34**(13), 5337–5346.
  - 5 (a) K. Domen, A. Kudo, A. Shinozaki, A. Tanaka, K. Maruya and T. Onishi, *J. Chem. Soc., Chem. Commun.*, 1986, 356–357; (b) A. Kudo, A. Tanaka, K. Domen, K. Maruya, K. Aika and T. Onishi, *J. Catal.*, 1988, **111**, 67–76; (c) Y. Miseki and A. Kudo, *ChemSusChem*, 2011, **4**, 245–251.
  - 6 (a) Z. Zhang, Q. Lin, D. Kurunthu, T. Wu, F. Zuo, S.-T. Zheng, C. J. Bardeen, X. Bu and P. Feng, *J. Am. Chem. Soc.*, 2011, **133**, 6934–6937; (b) P. Huang, C. Qin, Z.-M. Su, Y. Xing, X.-L. Wang, K.-Z. Shao, Y.-Q. Lan and E.-B. Wang, *J. Am. Chem. Soc.*, 2012, **134**, 14004–14010; (c) Z.-L. Wang, H.-Q. Tan, W.-L. Chen, Y.-G. Li and E.-B. Wang, *Dalton Trans.*, 2012, **41**, 9882–9884.
  - 7 J.-H. Son, C. A. Ohlin and W. H. Casey, *Dalton Trans.*, 2012, **41**, 12674–12677.
  - 8 (a) B. W. Dale and M. T. Pope, *Chem. Commun.*, 1967, 792; (b) B. W. Dale, J. M. Buckley and M. T. Pope, *J. Chem. Soc. A*, 1969, 301–304; (c) C. M. Flynn Jr. and G. D. Stucky, *Inorg. Chem.*, 1969, **8**, 332–334; (d) C. M. Flynn Jr. and G. D. Stucky, *Inorg. Chem.*, 1969, **8**, 335–344; (e) J.-H. Son and W. H. Casey, *Dalton Trans.*, 2013, **42**, 13339–13342.
  - 9 (a) R. D. Shannon and C. T. Prewitt, *Acta Crystallogr., Sect. B: Struct. Crystallogr. Cryst. Chem.*, 1969, **25**, 925–945; (b) R. D. Shannon, *Acta Crystallogr., Sect. A: Cryst. Phys., Diffraction, Theor. Gen. Cryst.*, 1976, **32**, 751–767.
  - 10 F. A. Cotton, G. Wilkinson, C. A. Murillo and M. Bochmann, *Advanced Inorganic Chemistry*, Wiley-Interscience, New York, 6th edn, 1999.
  - 11 J. M. D. Coey, *Magnetism and Magnetic Materials*, Cambridge University Press, 2010.
  - 12 H. Liu, C. J. Gómez-García, J. Peng, J. Sha, Y. Li and Y. Yan, *Dalton Trans.*, 2008, 6211–6218.
  - 13 Q. S. Yin, J. M. Tan, C. Besson, Y. V. Geletii, D. G. Musaev, A. E. Kuznetsov, Z. Luo, K. I. Hardcastle and C. L. Hill, *Science*, 2010, **328**, 342–345.
  - 14 J.-H. Son, J. Wang, F. E. Osterloh, P. Yu and W. H. Casey, *Chem. Commun.*, 2014, **50**, 836–838.
  - 15 A. Kudo, K. Sayama, A. Tanaka, K. Asakura, K. Domen, K. Maruya and T. Onishi, *J. Catal.*, 1989, **120**, 337–352.
  - 16 (a) A. Furube, T. Shiozawa, A. Ishikawa, A. Wada, K. Domen and C. Hirose, *J. Phys. Chem. B*, 2002, **106**, 3065–3072; (b) A. G. S. Prado, L. B. Bolzon, C. P. Pedroso, A. O. Moura and L. L. Costa, *Appl. Catal., B*, 2008, **82**, 219–224.
  - 17 T. K. Townsend, N. D. Browning and F. E. Osterloh, *Energy Environ. Sci.*, 2012, **5**, 9543–9550.
  - 18 J. W. Vickers, H. Lv, J. M. Sumlin, G. Zhu, Z. Luo, D. G. Musaev, Y. V. Geletii and C. L. Hill, *J. Am. Chem. Soc.*, 2013, **135**, 14110–14118.

